Electrochemistry Communications 123 (2021) 106914

Contents lists available at ScienceDirect

Electrochemistry Communications

journal homepage: www.elsevier.com/locate/elecom

Laser induced graphene sensors for assessing pH: Application to wound management

Robert Barber [a], Sarah Cameron [a,b], Amy Devine [a], Andrew McCombe [a], L. Kirsty Pourshahidi [b], Jill Cundell [c], Souradeep Roy [d], Ashish Mathur [e], Charnete Casimero [a], Pagona Papakonstantinou [a], James Davis [a,*]

[a] School of Engineering, Ulster University, Jordanstown, United Kingdom
[b] School of Biomedical Sciences, Ulster University, Coleraine, United Kingdom
[c] School of Health Sciences, Ulster University, Coleraine, United Kingdom
[d] Amity Institute of Nanotechnology, Amity University, Uttar Pradesh, India
[e] Department of Physics, University of Petroleum and Energy Studies, Bidholi Campus, Dehradoon, India

ARTICLE INFO

Keywords:
Electrodes
Laser induced graphene
LIG
pH
Riboflavin
Wound

ABSTRACT

The laser-induced modification of polyimide substrates to yield conductive graphitised tracks sensitive to the solution pH is investigated. The influence of laser output and operating characteristics on the surface morphology and the consequential impact on electrochemical properties have been evaluated. Several sensor formats have been pursued using both potentiometric and voltammetric methodologies and found to provide a stable means of determining pH. While the potentiometric system was found to provide sub-Nernstian responses, the voltammetric system employing a riboflavin (vitamin B2) redox probe was found to exhibit classic Nernstian profiles (56 mV/pH). The versatility of the laser patterning on polyimide is shown to yield a mechanically flexible double-sided probe that could be suitable for use in a wide variety of clinical applications.

1. Introduction

The significance of point-of-care diagnostics in wound management, particularly those involving chronic (slow healing) wounds, has long been recognised, with the ability to acquire data on the dynamics of key biomarkers offering the ability to adjust treatment and thereby improve clinical outcomes. One of the key findings in the recent World Union of Wound Healing Societies' report: 'Diagnostics and Wounds: A Consensus Document' was that "diagnostic tools need to be moved into the clinic or the patient's home to ensure optimal care is provided for patients with wounds" [1]. The latter was supported by Dowsett and coworkers (2014) who found that, in the UK, the majority of patients with chronic wounds are treated within the community [2]. There are however substantial challenges (procedural and technical) to be overcome in order to produce robust sensors for use within clinical and/or domestic environments. Direct integration of any proposed sensor within conventional dressings that need frequent changes necessitates that it is disposable and hence inexpensive to manufacture. The aim of this study has been to investigate the performance of laser-induced graphene (LIG) as a possible sensing substrate for monitoring pH and to consider its potential applicability within wound environments.

The maintenance of a moist wound environment has long been established as a key tenet of wound care practices [3–6] where hydration at the wound bed is critical to facilitating the myriad of biochemical pathways responsible for enhancing the rate of wound healing [3–8]. It must be noted however that too much moisture at the wound site can induce moisture-associated skin damage (MASD), which will significantly delay the healing processes and thus a delicate balance is needed to avoid further clinical complications [9]. The inflammatory stage in wound healing is normally transient in acute wounds, but in chronic wounds can be non-resolving and the resulting exudate can be a major contributor to MASD [7–9]. The presence of excess exudate has been described as a "wounding" agent itself, where the prolonged action of proteases, neutrophils and pro-inflammatory cytokines within the exudate can greatly impede the normal healing transition stages and wound closure [10,11]. It is little surprise that delays in wound healing can significantly increase the risk of infection resulting in limb- and life-threatening consequences [7–11].

* Corresponding author.
E-mail address: james.davis@ulster.ac.uk (J. Davis).

https://doi.org/10.1016/j.elecom.2020.106914
Received 13 December 2020; Received in revised form 26 December 2020; Accepted 29 December 2020
Available online 5 January 2021

The need to monitor wound moisture is now recognised [12–14] and, from a clinical practice perspective, it could be envisaged that the availability of a sensor that can report wirelessly to the patient, nurse or healthcare assistant could enable the speedy replacement of the dressing such that MASD is minimised [15,16]. Connolly and colleagues were among the first to address this need and pioneered the Woundsense® system [17,18]. The device is based on a disposable sensing strip (composed of two silver chloride electrodes) that is embedded within a conventional wound dressing. The measurement is based on ac impedance recordings, which can yield dashboard information on the moisture content within the gauze dressing. However, there are two core limitations of the system, as presently specified. First, the sensor is not wireless and therefore requires user intervention for each measurement. Second, although it measures moisture content, it does not determine the pH of the fluid. The latter is significant as wound fluid pH has been identified as a key parameter in wound healing and its measurement could provide important insights into healing progress.

Graphene-based electrodes have been used in a myriad of sensing roles, but it is only in recent years that laser processing of polyimide (Kapton) has enabled the production of prepatterned graphene-like structures on previously insulating substrates. Numerous studies have investigated the use of LIG devices for a wide variety of purposes [19–23] but this report is the first to consider its application to pH sensors employing potentiometric and voltammetric transduction. In the case of the latter, riboflavin, vitamin B2, is employed as a pH-sensitive redox probe which can be applied to the LIG substrate. The optimisation of LIG electrode production is considered and the performance of the resulting sensors for determining pH is critically assessed.

2. Experimental details

All reagents were of the highest grade available and obtained from Sigma-Aldrich. Buffer solutions were typically Britton Robinson (BR), composed of equimolar acetic, boric, and phosphoric acids (each 0.04 M). These were adjusted to the required pH through the addition of sodium hydroxide. Electrochemical measurements were conducted using a micro Autolab (Type III) potentiostat using either a three-electrode configuration with glassy carbon (3 mm diameter, BAS Technicol), or laser scribed polyimide film serving as the working electrode. A platinum counter electrode and an Ag|AgCl half-cell reference electrode (3 M NaCl) completed the cell arrangement. All measurements were conducted at 22 °C ± 2 °C. Raman spectroscopy was conducted using a Renishaw Raman Microscope (20× objective lens) with a 532 nm laser operating at 10% power. Conductivity measurements of the lasered polyimide were acquired with a 4-point probe using a 2461 series SourceMeter® (Keithley). A number of laser systems were initially evaluated and included a NEJE 1500 mW diode laser engraver (DK-BL) and a ULS VLS2.30 25 W CO_2 laser cutter. The latter was used for the majority of investigations involving scribed polyimide (125 μm thick Kapton, Goodfellow Research Materials). Electrode substrates were sealed thermally in polyester laminate sheathes (125 μm, Rexel UK) containing a prepatterned window (2.5 mm × 2.5 mm) in order to define the geometric area of the electrode, as previously described [24].

3. Results and discussion

Scanning electron micrographs detailing the morphology of the lasered polyimide (PI) produced by a low-power diode laser are shown in Fig. 1. While the unmodified PI film is smooth and essentially featureless, laser ablation results in the production of furrow-like carbon foam structures. The action of localised heat leads to degradation of the polymer, resulting in the release of gas. This initially causes the polymer to foam and then cools to yield the raised carbonised track [19–23]. There is a large degree of heterogeneity associated with the structures.

The foam-like structures resulting from the imposition of the CO_2 laser at two different power settings of 7.5 W and 12.5 W are compared

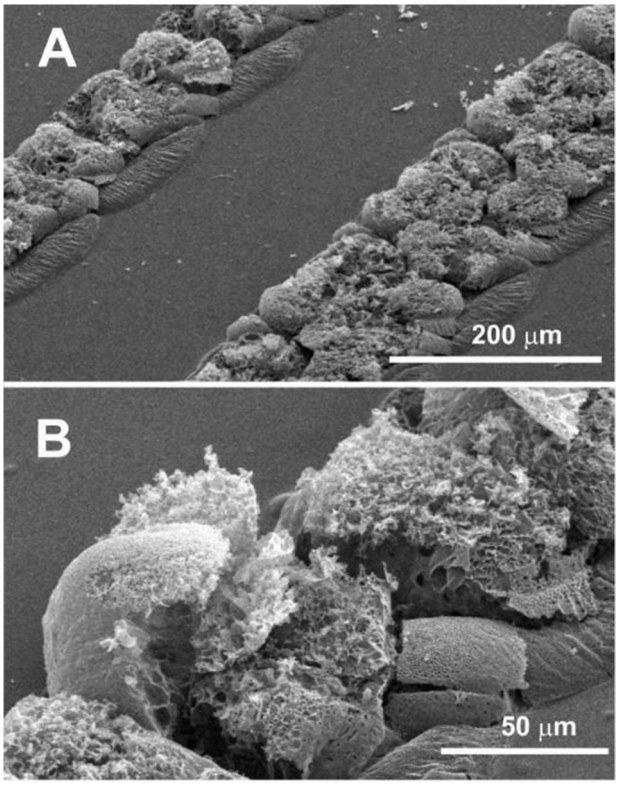

Fig. 1. SEM images of lasered polyimide tracks produced through the use of a 1.5 W diode laser.

in Fig. 2 and, in contrast to the structures produced by the diode laser, their morphology is consistent along the length of the track. At lower power settings (less than 5 W) using the same raster speed, less energy is deposited on the irradiated area due to a reduction in laser fluence. The conversion of polyimide to LIG is therefore not complete. It was observed that a power of 7.5 W, raster speed of 50.8 cm/s at 1000 pulses per inch (PPI) achieved good graphitisation and resulted in a homogenously porous web-like structure. Increasing the laser power beyond 7.5 W, the resulting LIG self-assembled into fibrous structures (with an average width of 216 nm at 12.5 W power) protruding upwards from the polyimide surface. This morphology was consistent with the laser-induced graphene fibers observed by the Tour group [23].

Multiple lasing of the same surface has previously been shown to be useful in improving the graphitisation of non-polyimide carbon precursor materials, thereby improving the conductivity of the fabricated LIG [25]. This was demonstrated in polyetherimide and organic material. Multiple lasing of the same area of polyimide did not induce an observable difference in the LIG morphology. It is hypothesised that the initial laser pass had sufficient fluence to photothermally break the carbon–gas bonds within the polyimide surface. The liberation of these gases caused the formation of the porous and fibrous morphology. Further laser passes only resulted in minor changes in the defective carbon structure due to graphitisation of small amounts of unconverted polyimide or due to thermal deterioration.

While both the diode and CO_2 systems yield conductive tracks, the greater uniformity of the carbonised tracks formed via the latter method was viewed as a more viable route to the production of reproducible electrode substrates for use in the subsequent investigations. Increasing the laser power can lead to greater carbonisation and, as a consequence, a greater degree of conductivity. Four probe conductivity measurements revealed that while the conductivity increases initially, it quickly plateaus beyond 7.5 W with an average of 444 S/m.

Raman spectra obtained from both the diode and CO_2 laser are

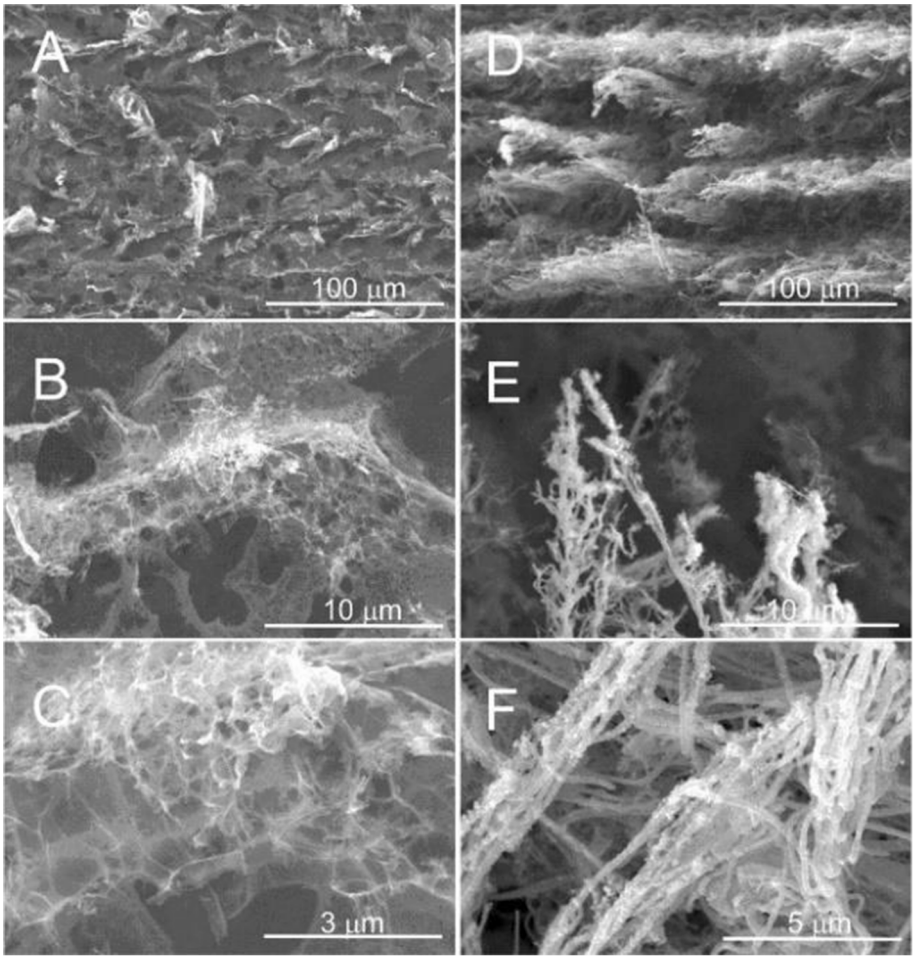

Fig. 2. SEM images of lasered polyimide tracks produced at a power of 7.5 W (A–C) and 12.5 W (D–F).

shown in Fig. 3 and exhibited the expected D and G peaks characteristic of a graphitic structure at 1350 and 1585 cm^{-1}, respectively. The D band originates from the carbon aromatic rings vibrating in a breathing mode with A1g symmetry and is a measure of the defective structure of the material. The G band is caused by in-plane sp^2 carbon atoms vibrating in a stretching mode with E2g symmetry [26,27].

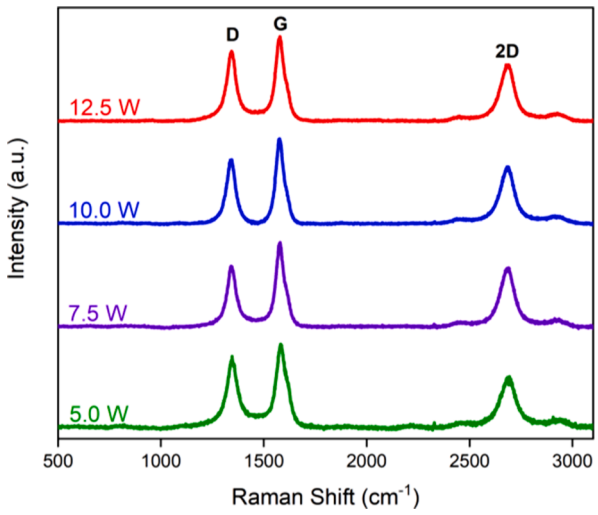

Fig. 3. Raman spectra of laser-induced graphene strips produced at different laser powers (5–12.5 W) and at a raster speed of 50.8 cm/s.

Raman spectra obtained from CO_2 laser irradiation displayed a strong D peak, an indication of high defect concentration, characteristic of defective graphene. SEM confirmed the abundance of defects in LIG caused by the porous morphology giving rise to many edges. The electron-rich defect edges facilitate the swift electron transfer observed in the fabricated sensor [28]. The sharp 2D peak confirmed that the polyimide film had been successfully graphitized and had formed a small number of graphene layers [23].

Cyclic voltammograms comparing the response of the LIG substrates (obtained at different power settings) and a conventional glassy carbon electrode towards ferrocyanide (2 mM, 0.1 M KCl, 50 mV/s) are detailed in Fig. 4. It can be seen that the laser power used to scribe the polyimide film had a considerable influence on the nature of the voltammograms obtained. It was observed that 7.5 W power yielded the classical reversible behaviour expected for the ferrocyanide couple (ΔEp: 67 mV). The latter can be attributed to the greater disorder of the graphitic lattice (as corroborated by the Raman spectra) producing more edge planes and increased surface oxygen functionalities. It is noteworthy that the LIG substrates produced by the 1.5 W diode laser did not yield any significant electrochemical response, indicating incomplete graphitisation. Examination of the 6.3 W and 12.5 W LIG responses shows contrasting behaviour, with 6.3 W highlighting the onset of electrochemically viable substrates and the 12.5 W setting indicating that excessive ablation can lead to substantive deterioration in the performance (ΔEp: >100 mV). The latter is also characterised by a change in the morphology of the LIG substrate, where a more fibrous structure is observed (Fig. 2D–F). There is clearly an optimum configuration for the production of electrodes, with subtle variations in power (i.e. from 6.3 W to 12.5 W) yielding

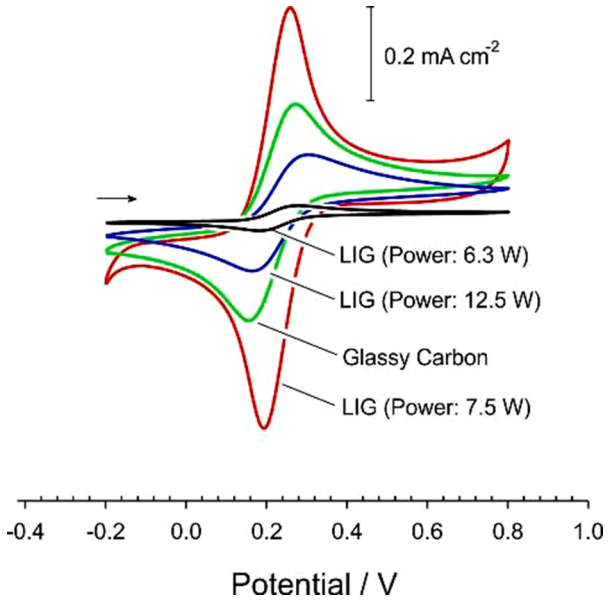

Fig. 4. Cyclic voltammograms comparing the responses of glassy carbon and laser-scribed polyimide electrodes towards ferrocyanide (2 mM, 0.1 M KCl, 50 mV/s).

considerable differences in performance. Given such sensitivity and the variations in the design and operating conditions of individual laser systems, it is critical that some form of pre-calibration is considered prior to the manufacture of LIG substrates.

3.1. Response to pH

A simple potentiometric model employing LIG electrodes was initially proposed on the grounds that any clinical implementation would have to possess both a small, unobtrusive electronic area and a low power requirement. A dual electrode array employing two parallel LIG tracks was adopted with silver paint deposited at the terminus of one as indicated in the inset within Fig. 5. The latter was to serve as a solid-state silver-silver chloride pseudo reference. The main tracks were then sealed within a thermal laminate to define the sensing and connection ends. The potential difference between the uncoated LIG and the silver-coated LIG was used as the basis of the analytical signal. The sensor was placed within Britton Robinson buffers of known pH (in the range pH 3 to pH 8) with 0.1 M KCl as the supporting electrolyte. The potential difference was recorded over a period of 5 min and the average potential over the last 10 s used as the datum point. The results are summarised in Fig. 6, where the data refers to the three replicate measurements. The response was found to be stable, with minimal drift between replicates, and yields a sub-Nernstian pH profile ($E/V = 0.038$ pH $+ 0.359$; $N = 18$; $R^2 = 0.996$).

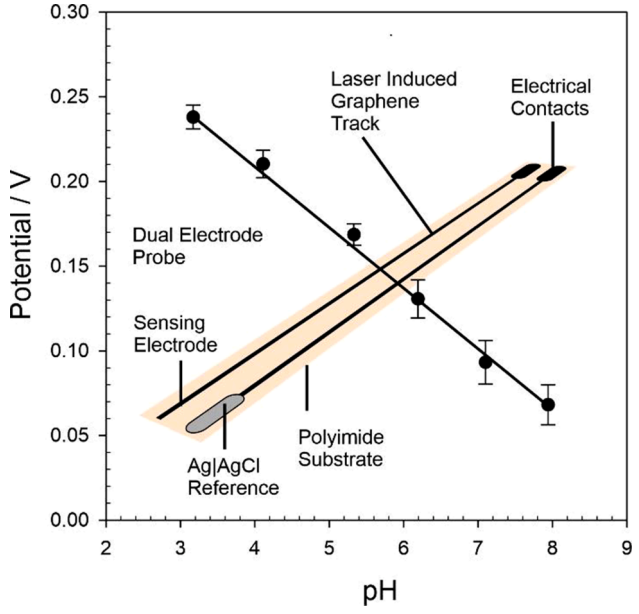

Fig. 5. Influence of pH on the potential difference recorded at the dual electrode laser-induced graphene sensing array (Inset).

An alternative design was also evaluated where the LIG electrodes were formed on either side of the same polyimide layer, as indicated in Fig. 6**.** In this iteration, the LIG tracks essentially mirror one another but are separated by the layer of non-lasered, non-conductive polyimide. While the polyimide is mechanically flexible, the physical breadth of the system in which the electrodes are positioned parallel to one another on the same substrate could be an impediment for wounds occurring near the joints or between the toes. The core advantage of this new approach was to reduce the lateral dimensions of the probe to a width of less than 2 mm, thereby enabling the sensor to be used in more demanding wound environments.

The dual-sided probe performance was assessed under similar conditions to those used previously with the parallel LIG design covering the same pH buffer range. As with the parallel LIG tracks, a sub Nernstian ($E/V = 0.024$ pH $+ 0.118$; $N = 6$; $R^2 = 0.985$) response was observed. It is clear that the laser ablation on either side of the polyimide substrate can be achieved without burn-through and can yield sensors with a smaller physical footprint. The sub-Nernstian response is however problematic from a sensitivity perspective and, as such, an alternative detection strategy was required.

The use of voltammetry for the measurement of pH has gained considerable interest in recent years, as it offers a faster and more robust response. Various quinone systems have been used in this context [29–35] but few would be considered suitable for use within a wound environment. To counter issues of biocompatibility, riboflavin (vitamin B2) was employed and its response to varying pH conditions at the LIG based sensors evaluated. The pH dependence of riboflavin's redox transitions are highlighted in Fig. 7 and it could be envisaged that the potential of the oxidation peak process (I− > II) could be used as the basis of an indirect measure of pH [35]. As in previous reports on the application of voltammetry to the measurement of pH [29–39], square-wave voltammetry was employed in order to improve the determination of the peak potentials [35]. The typical responses of a LIG electrode towards riboflavin (3.2 mM) in various buffers (pH 2.8–8) are detailed in Fig. 7. The oxidation peak position was found to shift with increasing pH to more negative potentials, with a near-Nernstian shift ($E/V = 0.056$ pH $+ 0.053$; $N = 18$; $R^2 = 0.991$) with pH.

It has long been recognised that the presence of quinone groups at the interface of carbon electrodes can give rise to a potentiometric response and that the population of these redox groups can be increased through oxidative processing of the electrode material [40]. It would be expected that the ablation of the polyimide here would similarly lead to

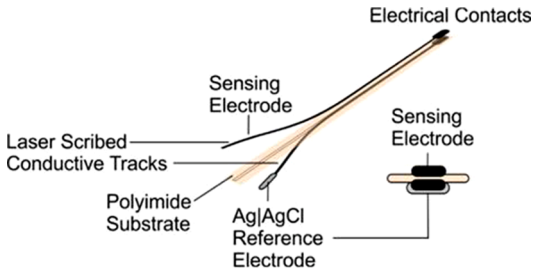

Fig. 6. Schematic of the double-sided laser-induced graphene polyimide probe.

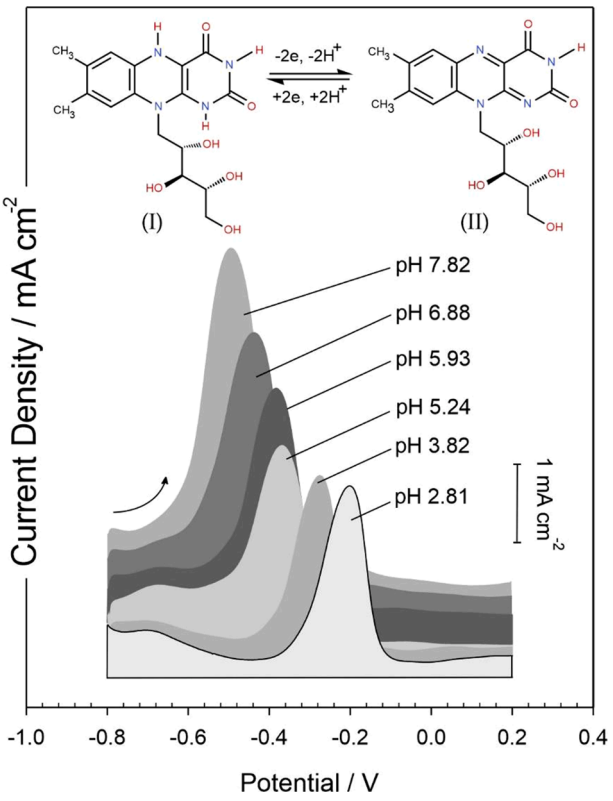

Fig. 7. Square-wave voltammograms detailing the influence of pH on the response of the laser-scribed electrode towards riboflavin (3.2 μM) in Britton Robinson buffers.

the generation of pH-sensitive quinone moieties and this was observed in the voltammetric profiles (highlighted in more detail in Fig. S1). Work by Paixao et al. (2002) has shown that electrochemically pre-treated glassy carbon electrodes can serve as pH sensors in potentiometric titrations [41] and it is possible to speculate that quinone species within the oxidised carbon backbone are integral to the potentiometric response (Fig. 5). In contrast to conventional ion-selective electrodes, there is no single, defined, redox couple responsible for the signal, and particularly in this instance, the LIG surface is liable to be a heterogeneous collection of redox groups possessing various acid–base functionalities. This is corroborated by the broad quinone peak processes shown in Fig. S1. Lu et al. (2014) have also demonstrated the utility of exploiting the quinone groups in glassy carbon electrodes as voltametric pH sensors [38] but in the present case, the peak current magnitude of the intrinsic quinone redox process was found to be less than 5% of that of the riboflavin system and clearly highlights the advantage of employing the latter as a pH-sensitive redox probe. A comparison of the present work with recent advances in voltammetric pH sensing systems is given in Table 1.

4. Conclusions

Laser-scribed polyimide has been shown to serve as an inexpensive substrate for the measurement of pH through two detection methodologies. Potentiometric detection provides a simple, reagentless approach to pH measurement but while robust, exhibits a sub-Nernstian response that will severely limit the sensitivity of the system. The voltammetric approach, in contrast, exploits the pH dependence of a riboflavin redox indicator and yields a well-defined voltammetric peak profile that shifts in a Nernstian manner with changes in pH. The mechanically flexible nature of the underpinning substrate, its ease of manufacture, small dimensions and clear response to pH could serve as the foundations for a range of sensors with clinical applications. Significantly, the ability to selectively pattern the polyimide substrate through the use of the laser offers an exceedingly versatile approach to additive manufacture and the rapid prototyping of new sensor designs.

Table 1
Alternative voltammetric pH sensing systems.

Electrode Modifier	mV/pH	Ref
Ferrocene/dyad	52	[30]
Anthraquinone/diphenyl - phenylenediamine	114	[31]
Polyplumbagin	51	[32]
Nafion/benzoquinone	59	[33]
Uric Acid	62	[36]
Ferrocene / phenanthraquinone	97	[34]
Polyflavin film	57	[35]
Carbon-quinones	57	[37]
Unmodified glassy carbon	61	[38]
Iridium oxide	121	[39]
Riboflavin	56	This work

Declaration of Competing Interest

The authors declare that they have no known competing financial interests or personal relationships that could have appeared to influence the work reported in this paper.

Acknowledgments

The authors acknowledge financial support from the European Union's INTERREG VA Programme, managed by the Special EU Programmes Body (SEUPB), the Department for the Economy (DfE) Northern Ireland, Kimal PLC, Abbott Diabetes Care Inc. and the British Council UKIERI (DST 65/2017).

Appendix A. Supplementary data

Supplementary data to this article can be found online at https://doi.org/10.1016/j.elecom.2020.106914.

References

[1] K. Harding, Principles of Best Practice: Diagnostics and Wounds, A Consensus Document,World Union of Wound Healing Societies (WUWHS), London, 2008.
[2] C. Dowsett, A. Bielby, R. Searle, Reconciling increasing wound care demands with available resources, J. Wound Care 23 (2014) 552–562, https://doi.org/10.12968/jowc.2014.23.11.552.
[3] G.D. Winter, Effect of air exposure and occlusion on experimental human skin wounds, Nature 200 (1963) 378–379.
[4] G.D. Winter, Effect of air drying and dressings on the surface of the wound, Nature 197 (1963) 91–92.
[5] G.D. Winter, Formation of the scab and the rate of epithelization of superficial wounds in the skin of the young domestic pig, Nature 193 (1962) 293–294, https://doi.org/10.1038/193293a0.
[6] G.D. Winter, A note on wound healing under dressings with special reference to perforated-film dressings, J. Invest. Dermatol. 45 (1965) 299–302.
[7] G.A. Kannon, A.B. Garrett, Moist wound healing with occlusive dressings: a clinical review, Dermatologic Surg. 21 (1995) 583–590, https://doi.org/10.1111/j.1524-4725.1995.tb00511.x.
[8] M.G. Rippon, K. Ousey, K.F. Cutting, Wound healing and hyper-hydration: a counterintuitive model, J. Wound Care 25 (2016) 68–75, https://doi.org/10.12968/jowc.2016.25.2.68.
[9] H. Haryanto, D. Arisandi, S. Suriadi, I. Imran, K. Ogai, H. Sanada, M. Okuwa, J. Sugama, Relationship between maceration and wound healing on diabetic foot ulcers in Indonesia: a prospective study, Int. Wound J. 14 (2017) 516–522, https://doi.org/10.1111/iwj.12638.
[10] K. Moore, Cell biology of normal and impaired healing, in: S. Percival, K. Cutting (Eds.), Microbiology of Wounds, CRC PRess, 2010.
[11] J. Chen, Aquacel Hydrofibre Dressings: The Next Step in Wound Dressing Technology, London, 1998.
[12] L.A. Schneider, A. Korber, S. Grabbe, J. Dissemond, Influence of pH on wound-healing: a new perspective for wound-therapy? Arch. Dermatol. Res. 298 (2007) 413–420, https://doi.org/10.1007/s00403-006-0713-x.
[13] C. Scott, S. Cameron, J. Cundell, A. Mathur, J. Davis, Adapting resistive sensors for monitoring moisture in smart wound dressings, Curr. Opin. Electrochem. 23 (2020) 31–35, https://doi.org/10.1016/j.coelec.2020.02.017.

[14] A. McLister, J. McHugh, J. Cundell, J. Davis, New developments in smart bandage technologies for wound diagnostics, Adv. Mater. 28 (2016) 5732–5737, https://doi.org/10.1002/adma.201504829.
[15] C. Dowsett, Exudate management: a patient-centred approach, (n.d.) 249–252.
[16] P. Drew, J. Posnett, L. Rusling, The cost of wound care for a local population in England, Int. Wound J. 4 (2007) 149–155, https://doi.org/10.1111/j.1742-481X.2007.00337.x.
[17] D. McColl, B. Cartlidge, P. Connolly, Real-time monitoring of moisture levels in wound dressings in vitro: an experimental study, Int. J. Surg. 5 (2007) 316–322, https://doi.org/10.1016/j.ijsu.2007.02.008.
[18] S.D. Milne, I. Seoudi, H. Al Hamad, T.K. Talal, A.A. Anoop, N. Allahverdi, Z. Zakaria, R. Menzies, P. Connolly, A wearable wound moisture sensor as an indicator for wound dressing change: an observational study of wound moisture and status, Int. Wound J. 13 (2016) 1309–1314, https://doi.org/10.1111/iwj.12521.
[19] S.P. Singh, Y. Li, A. Be'Er, Y. Oren, J.M. Tour, C.J. Arnusch, Laser-induced graphene layers and electrodes prevents microbial fouling and exerts antimicrobial action, ACS Appl. Mater. Interfaces 9 (2017) 18238–18247, https://doi.org/10.1021/acsami.7b04863.
[20] L. Li, J. Zhang, Z. Peng, Y. Li, C. Gao, Y. Ji, R. Ye, N.D. Kim, Q. Zhong, Y. Yang, H. Fei, G. Ruan, J.M. Tour, High-performance pseudocapacitive microsupercapacitors from laser-induced graphene, Adv. Mater. 28 (2016) 838–845, https://doi.org/10.1002/adma.201503333.
[21] D.X. Luong, A.K. Subramanian, G.A.L. Silva, J. Yoon, S. Cofer, K. Yang, P.S. Owuor, T. Wang, Z. Wang, J. Lou, P.M. Ajayan, J.M. Tour, Laminated object manufacturing of 3D-printed laser-induced graphene foams, Adv. Mater. 30 (2018) 1–6, https://doi.org/10.1002/adma.201707416.
[22] J. Lin, Z. Peng, Y. Liu, F. Ruiz-Zepeda, R. Ye, E.L.G.G. Samuel, M.J. Yacaman, B. I. Yakobson, J.M. Tour, Laser-induced porous graphene films from commercial polymers, Nat. Commun. 5 (2014) 5714, https://doi.org/10.1038/ncomms6714.
[23] L.X. Duy, Z. Peng, Y. Li, J. Zhang, Y. Ji, J.M. Tour, Laser-induced graphene fibers, Carbon N. Y. 126 (2018) 472–479, https://doi.org/10.1016/j.carbon.2017.10.036.
[24] J.S.N. Dutt, M.F. Cardosi, S. Wilkins, C. Livingstone, J. Davis, Characterisation of carbon fibre composites for decentralised biomedical testing, Mater. Chem. Phys. 97 (2006) 267–272, https://doi.org/10.1016/j.matchemphys.2005.08.021.
[25] Y. Chyan, R. Ye, Y. Li, S.P. Singh, C.J. Arnusch, J.M. Tour, Laser-Induced graphene by multiple lasing: toward electronics on cloth, paper, and food, ACS Nano 12 (2018) 2176–2183, https://doi.org/10.1021/acsnano.7b08539.
[26] Z. Gao, J. Zhu, S. Rajabpour, K. Joshi, M. Kowalik, B. Croom, Y. Schwab, L. Zhang, C. Bumgardner, K.R. Brown, D. Burden, J.W. Klett, A.C.T. van Duin, L.V. Zhigilei, X. Li, Graphene reinforced carbon fibers, Sci. Adv. 6 (2020), https://doi.org/10.1126/sciadv.aaz4191 eaaz4191.
[27] F. Rosenburg, E. Ionescu, N. Nicoloso, R. Riedel, High-temperature Raman spectroscopy of nano-crystalline carbon in silicon oxycarbide, Materials (Basel) 11 (2018) 93, https://doi.org/10.3390/ma11010093.
[28] J. Benson, Q. Xu, P. Wang, Y. Shen, L. Sun, T. Wang, M. Li, P. Papakonstantinou, Tuning the catalytic activity of graphene nanosheets for oxygen reduction reaction via size and thickness reduction, ACS Appl. Mater. Interfaces 6 (2014) 19726–19736, https://doi.org/10.1021/am5048202.
[29] G.J. Tustin, V.G.H. Lafitte, C.E. Banks, T.G.J. Jones, R.B. Smith, J. Davis, N. S. Lawrence, Synthesis and characterisation of water soluble ferrocenes: molecular tuning of redox potentials, J. Organomet. Chem. 692 (2007) 5173–5182, https://doi.org/10.1016/j.jorganchem.2007.07.048.
[30] W. Park, S. Kim, Triggerable single-component two-electrode voltammetric pH sensors using dyad molecules, Electrochem. Commun. 26 (2013) 109–112, https://doi.org/10.1016/j.elecom.2012.10.025.
[31] I. Streeter, H.C. Leventis, G.G. Wildgoose, M. Pandurangappa, N.S. Lawrence, L. Jiang, T.G.J. Jones, R.G. Compton, A sensitive reagentless pH probe with a ca. 120 mV/pH unit response, J. Solid State Electrochem. 8 (2004) 718–721, https://doi.org/10.1007/s10008-004-0536-7.
[32] J. Davis, M.T. Molina, C.P. Leach, M.F. Cardosi, Plasma-polyplumbagin-modified microfiber probes: a functional material approach to monitoring vascular access line contamination, ACS Appl. Mater. Interfaces 5 (2013), https://doi.org/10.1021/am402821c.
[33] R.A. Webster, F. Xia, M. Pan, S. Mu, S.E.C. Dale, S.C. Tsang, F.W. Hammett, C. R. Bowen, F. Marken, Voltammetric probing of pH at carbon nanofiber-NafionTM-carbon nanofiber membrane electrode assemblies, Electrochim. Acta 62 (2012) 97–102, https://doi.org/10.1016/j.electacta.2011.11.095.
[34] A.E. Musa, M.A. Alonso-Lomillo, F.J. Del Campo, N. Abramova, O. Domínguez-Renedo, M.J. Arcos-Martínez, J.P. Kutter, Thick-film voltammetric pH-sensors with internal indicator and reference species, Talanta 99 (2012) 737–743, https://doi.org/10.1016/j.talanta.2012.07.014.
[35] C. Casimero, A. McConville, J.J. Fearon, C.L. Lawrence, C.M. Taylor, R.B. Smith, J. Davis, Sensor systems for bacterial reactors: a new flavin-phenol composite film for the in situ voltammetric measurement of pH, Anal. Chim. Acta 1027 (2018) 1–8, https://doi.org/10.1016/j.aca.2018.04.053.
[36] J. Phair, L. Newton, C. McCormac, M.F. Cardosi, R. Leslie, J. Davis, A disposable sensor for point of care wound pH monitoring, Analyst 136 (2011) 4692, https://doi.org/10.1039/c1an15675f.
[37] C. Hegarty, A. McConville, R.J. McGlynn, D. Mariotti, J. Davis, Design of composite microneedle sensor systems for the measurement of transdermal pH, Mater. Chem. Phys. 227 (2019) 340–346, https://doi.org/10.1016/j.matchemphys.2019.01.052.
[38] M. Lu, R.G. Compton, Voltammetric pH sensing using carbon electrodes: glassy carbon behaves similarly to EPPG, Analyst 139 (2014) 4599–4605, https://doi.org/10.1039/C4AN00866A.
[39] K. Chaisiwamongkhol, C. Batchelor-McAuley, R.G. Compton, Optimising amperometric pH sensing in blood samples: an iridium oxide electrode for blood pH sensing, Analyst 144 (2019) 1386–1393, https://doi.org/10.1039/C8AN02238K.
[40] A. Anderson, J. Phair, J. Benson, B. Meenan, J. Davis, Investigating the use of endogenous quinoid moieties on carbon fibre as means of developing micro pH sensors, Mater. Sci. Eng. C 43 (2014) 533–537, https://doi.org/10.1016/j.msec.2014.07.0380928-4931.
[41] T.R.L.C. Paixao, L. Kosminsky, M. Bertotti, Use of electrochemically pretreated glassy carbon electrodes as pH sensors in potentiometric titrations, Sens. Actuators B 87 (2002) 41–46, https://doi.org/10.1016/s0925-4005(02) 00201-0.